



## **RESPONSES OF THE CARQUINEZ, CALIFORNIA SUSPENSION BRIDGE DURING THE MW6.0 SOUTH NAPA EARTHQUAKE OF AUGUST 24, 2014**

M. Çelebi(1), S. F. Ghahari(2), and E. Taciroglu(3)

- (1) Senior Research Civil Engineer, USGS, Menlo Park, CA., USA, celebi@usgs.gov
- (2) Post-Doctoral Fellow, Univ. Calif. Los Angeles, Los Angeles, CA., USA, ghahari@gmail.com
- (3) Professor, Univ. Calif. Los Angeles, Los Angeles, CA., USA, etacir@ucla.edu

### ***Abstract***

The behavior of the suspension bridge in Carquinez, CA, during the Mw6.0 24 August 2014 South Napa, CA earthquake is studied using data recorded by an extensive array of accelerometers. Modes, corresponding frequencies and damping are identified and compared with previous studies that used ambient data of the deck only plus mathematical models. Data are systematically analyzed for vertical, transverse and torsional motions of the deck, and transverse, longitudinal and torsional motions of the towers. The transverse and vertical fundamental mode frequencies of the deck are the same (0.17Hz) due to coupling. Higher frequencies for transverse and vertical coupled modes are the same at 0.46Hz and 0.98Hz. Tower translational frequencies are 0.39Hz in the transverse direction and 0.46 Hz in the longitudinal direction, and are coupled with those of the deck. Coupling of torsional modes of the tower and deck are identified. A beating effect is observed, particularly for torsional motions.

*Keywords: Carquinez suspension bridge; Napa earthquake response; modal frequencies; modes.*



## 1. Introduction

The purpose of this paper is to highlight a study of the recorded strong-motion responses of the suspension bridge across Carquinez Strait (California) during the  $M_w=6.0$  24 August 2014 South Napa, CA earthquake (03:20:44 PDT; 38.22N, 122.31W., <http://earthquake.usgs.gov/earthquakes/eqarchives/poster/2014/20140824.php>, last accessed December 29, 2015) [hereafter referred to as Napa EQ], about 19.5 km NNW of the bridge. This bridge is one of two bridges spanning Carquinez Strait, herein labeled as the “Odd Couple” of bridges -an appropriate label since each bridge is of different design and age. The westbound suspension bridge identified by California Geological Survey (CGS) Station 68185 that opened to service in 2003 and known as the Alfred Zampa Memorial Bridge replaced an older 1927 construction cantilever truss bridge deemed seismically unsafe. Fig. 1a shows a map of the layout and Fig. 1b shows a picture of both of the two bridges. Adopted from [www.strongmotioncenter.org](http://www.strongmotioncenter.org) (last accessed January 4, 2016), Fig. 1c displays relative dimensions, vertical section and plan views of the suspension bridge as well as sensor locations and orientations, and Fig. 1d shows south elevation view of Tower T2 showing details of deck and rocker link. The azimuths of the two bridges are listed as  $358^\circ$  and  $357^\circ$  respectively at [www.strongmotioncenter.org](http://www.strongmotioncenter.org). The parallel bridges serve as main transportation lifelines on Interstate 80 connecting the San Francisco Bay area and the capital city of Sacramento, CA, as well as to Reno, NV, the well-known Napa Valley wine-country, and the rest of Northern California. The bridge was not damaged during the Napa EQ. However, the earthquake caused medium- to high-level damage to homes, businesses and other infrastructure in the epicentral area [1].

Only a small percentage of long-span bridges around the world have been permanently instrumented to capture their behavior (and performance) during significant shaking events. However, the behavior of many long-span bridges have been studied using data from temporary arrays deployed to record responses to ambient motions and (or) mathematical models. For example, ambient data from the Golden Gate Bridge (GGB), a well-known landmark of San Francisco, CA., were studied by Abdel-Ghaffar and Scanlan [2,3] [<http://www.goldengatebridge.org/projects/retrofit.php>, last accessed 10/18/2010], and Vincent [4,5,6]. The bridge was instrumented after the 1989 Loma Prieta (CA) earthquake ( $M_w6.9$ ). Earthquake responses of GGB were studied by Çelebi [7] using three sets of low-amplitude responses from three earthquakes. The two long-span suspension bridges in Istanbul have been instrumented and both ambient and earthquake response data have been captured (N. Apaydin, *pers. comm.* 2015). A long-span cable-stayed bridge in Cape Girardeau (MO) was studied using both ambient and earthquake data by Çelebi [8]. Siringoringo et al. [9] performed analyses of response data from the Yokohama Bay (Japan) bridge recorded during the  $M_w9.0$  Tohoku earthquake of 2011. Analyses were done separately for longitudinal, vertical and transverse directions and coupling of vertical and transverse modes were displayed. In an earlier paper, Siringoringo and Fujino [10] performed system identification and finite element analyses of the same bridge with numerous earthquake data sets and ambient vibration data. Reported results from both studies are similar.

Before opening to traffic, the Carquinez Bridge, subject matter of this paper, was studied extensively by other researchers using data from temporary arrays deployed only on the deck and using mathematical models [11-15]. They obtained multiple sets of ambient data from temporary deployment of 64 channels of accelerometers to measure the vertical, transverse and longitudinal motions of only the bridge deck to wind and forced vibration tests conducted during controlled traffic. They used different system identification methods, time-domain techniques, and finite element modeling to extract mode shapes and associated frequencies (e.g., symmetric horizontal transverse mode identified at  $\sim 0.1580.165$  Hz). Prior to these, Nayeri performed system identification studies on the data recorded by dynamic testing [16]. Similarly, Betti et al. [14] and Hong et al. [15] studied bridge behavior with multiple sets of ambient data obtained using the CSMIP array, as well as finite element modeling. Their results, while mostly similar to those determined by previous researchers, dwell on several modes that occur within a narrow frequency range. There is no discussion of response characteristics in terms of coupled modes or interaction between towers and deck via cables. Comparisons of results from this study will be made with those from prior studies.



Studies of the seismic behavior of long-span bridges are important (as are tall buildings and other types of structures) to understand their dynamic characteristics (modes and associated frequencies and damping, coupled or uncoupled mode shapes, unique modal aspects such as combinations of modes during shaking, and beating effects). In addition to determining behavioral characteristics, capturing response data is useful in assessing vulnerability and performances of structures. Such studies can lead to improved future designs and/or help to retrofit or strengthen existing ones.

In this current study, the aim is to understand the behavior of the Carquinez Strait suspension bridge during the 2014 South Napa earthquake. It should be pointed out that the 2014 South Napa earthquake records of the bridges are the first earthquake records from the arrays deployed at the two bridges. Studies using aftershock records of the South Napa earthquake or ambient test data are outside of the scope of this paper.

## 2. Suspension Bridge

Fig. 3 shows the relevant dimensions, sensor locations and orientations of the *suspension bridge*. The bridge is 1056 m long between Pier P1 and the north anchorage (Abutment A4). The center span between towers T2 and T3 of the bridge is 728 m. The south side span between Pier P1 and Tower T2 is 147 m, while the north side span between Tower T3 and the north anchorage is 181 m. In the north, the cables anchor at the end of the suspension span. In the south, the anchorage structure of the cables is 84m south of Pier P1 that serves as end of the suspension span. Pier 1 levels the roadway leading to the south with the north anchorage. The tops of towers T2 and T3 (Fig. 1d) are both ~ 74 m above deck level and ~ 112m and 118 m above their respective concrete pile caps that sit on top of 3m diameter cast in steel shell (CISS) piles<sup>1</sup>. Each tower has two concrete pylons 27 m apart that are connected with pre-stressed concrete struts at the top and below deck level. The deck is constructed with steel orthotropic box girders. The details of the support and design aspects of the tower, prestressed concrete struts (as well as very detailed design approaches and aspects of the bridge are in (<http://www.opacengineers.com/features/carquinez>, accessed December 14, 2015).

An important detail that is essential to data analyses described later in this paper is the rocker link-type support of the deck at both towers T2 and T3 (Fig. 1d). This type of support, resting on a pre-stressed concrete strut connecting the two columns of each of the towers, eliminates the relative vertical displacements of the steel box girder deck from the struts of each of the towers T2 and T3 - without constraining the rotations of the deck around the transverse axes but allowing very small transverse displacements of the deck (*pers. comm.* Pat Hipley, 2015).

In this study, moving window analyses and spectral analyses techniques including amplitude spectra, cross-spectra, phase spectra and coherency (e.g., [17]) are used to infer the behavior of important components of the bridge (e.g., center span deck and towers, T2 and T3). Predominant frequencies are inferred from peaks (by peak picking) of the amplitude spectra. As will be shown later, such inference by peak picking can result in an identical frequency for a coupled mode. However, system identification (SID) studies performed later in the paper reveal a small variation of the two frequencies of a coupled mode attributable to two different computational processes. Thus, for example, during SID, two close frequencies can be identified for closely coupled modes, whereas in spectral analyses, we infer and accept a single frequency for a coupled mode. For pragmatic reasons, both are correct. Mathematical modeling and finite element analyses are not performed in this study.

The moving-window analysis applied herein is commonly known as time-frequency distributions (TFDs) of recorded data. Moving window figures that follow display the TFDs obtained using the Smoothed Pseudo Wigner-Ville (SPWV) method [18]<sup>2</sup>.

---

<sup>1</sup> Data on number and depth of piles were not available.

<sup>2</sup> Wigner-Ville Distributions (WVD) are obtained in similar fashion as a short-time Fourier Transform, but the integration kernel comprises the instantaneous auto-correlation function of the input signal with respect to the delay/convolution variable. The SPWV distributions are improved versions of WVDs and alleviate cross-term interference. Here, we used the Time-Frequency Toolbox by Auger et al.[20] written for Matlab (Mathworks, 2013) to compute and plot the TFDs of recorded signals.

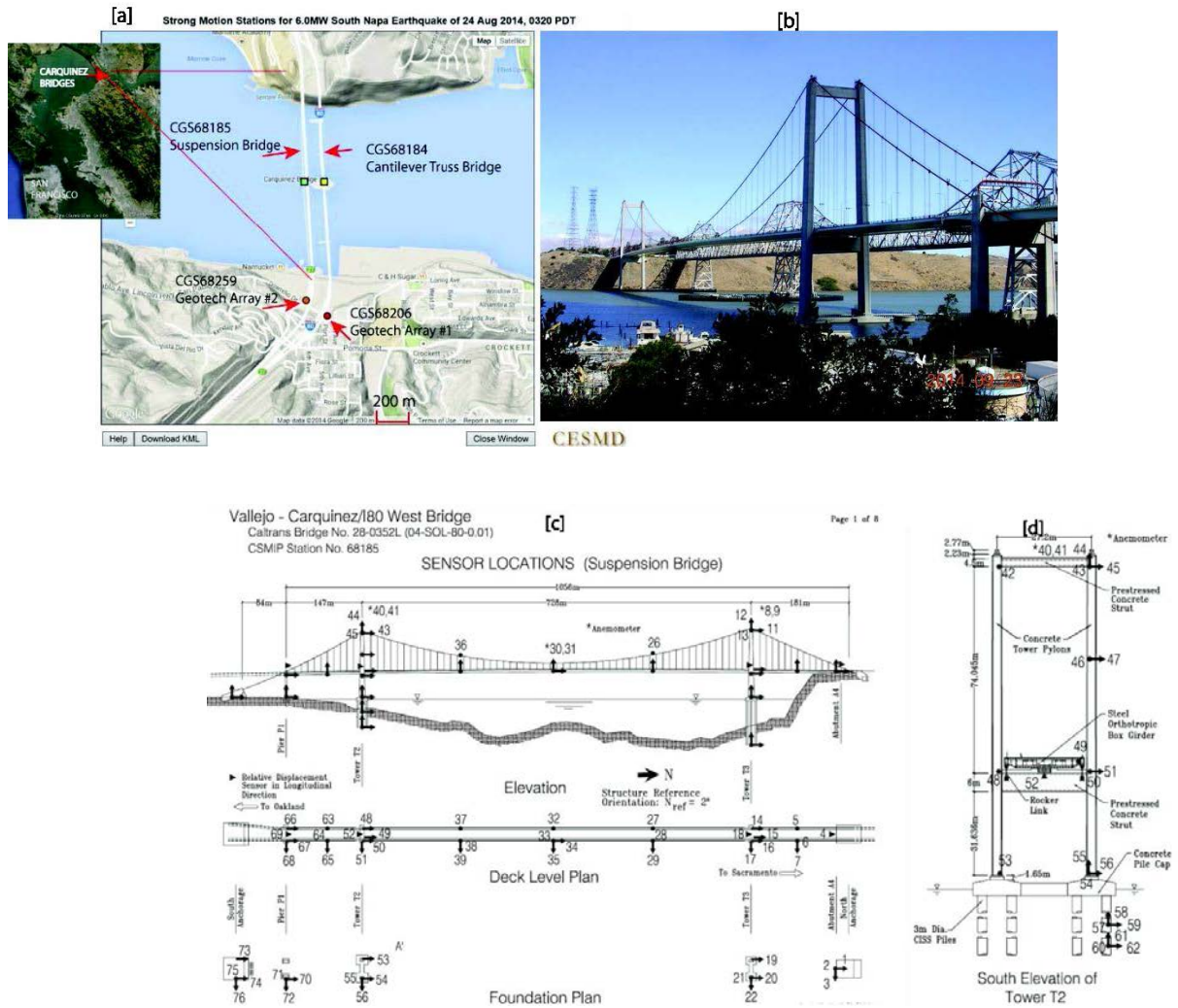


Fig. 1- (a) A Google Earth map showing the locations of Carquinez Strait bridges (w.r.t) San Francisco, CA and the locations of the two free-field surface and downhole arrays (base figure courtesy of Moh Huang [CGS]). Note the proximity of geotechnical arrays to the bridges. (b) Photo of the two parallel Carquinez Strait Bridges (courtesy of Moh Huang [CGS]). Both adopted from [www.strongmotioncenter.org](http://www.strongmotioncenter.org) (last accessed January 4, 2016), (c) Sensor locations and orientations, and relative dimensions of the suspension bridge and (d) South elevation view of Tower T2 showing details of deck and rocker link.

### 3. Instrumentation and Analyses of 24 August 2014 Napa EQ Data

The *suspension bridge* was instrumented by the California Strong Motion Instrumentation Program (CSMIP) of the California Geological Survey (CGS) in 2004 with 76 channels of accelerometers on the suspension bridge and 27 channels on approach structures<sup>3</sup>. The majority of the 76 channels deployed on the bridge, their locations

<sup>3</sup> In addition, it is important to note that a wireless monitoring system (named Narada) has been installed on the bridge with cooperative efforts of several institutions led by University of Michigan [21, 22]. However, because the system is set to record ambient data every two hours but not to record on a trigger threshold basis, the system did not record the response of the bridge during the 24 August 2014 mainshock.



and their orientations are displayed in Fig. 1c and 1d (adopted from the set of 8-page schematics in [www.strongmotioncenter.org](http://www.strongmotioncenter.org)). During the earthquake, 26 of the 76 channels did not record. This is significant because, for example, data from CH43 in the longitudinal direction at the top of T2 (where cables are attached) are important for analyzing the longitudinal and torsional behavior of T2. Despite missing some channels, the recorded data are utilized to identify transverse, vertical, longitudinal and torsional behavior of the bridge center span deck and towers. In general, side spans are not examined, although some plots include data from side spans for comparison.

The largest peak ground acceleration recorded at the suspension bridge (CGS Station 68185) was 0.15 g, while the largest peak structural accelerations were 0.60g (transverse on suspension cable CH26 and CH36), 0.32g (vertical at middle of deck center span (CH32 and CH33), and 0.31g (transverse at middle of deck center span CH35) ([www.strongmotioncenter.org](http://www.strongmotioncenter.org), Shakal et. al.[19], 2014). The largest peak displacements obtained by double integration of the accelerations at key locations of the suspension bridge are: mid-center span (vertical: 10.2cm, transverse: 8.6cm), towers (longitudinal at T2: 2.1cm and at T3: 2.1cm, transverse at T2: 6.3cm and at T3: 4.6cm). For a longspan bridge, these displacements are not large enough to infer possible damage. In any case, as mentioned earlier, no damage was observed.

Due to large amount of data, we present analyses of the transverse direction data in detail but limit the presentation of analyses of vertical and longitudinal data to minimal number of figures. Furthermore, mostly, we use only displacements (obtained from double integration of accelerations). It is important to note that studies by Siringoringa et al [9] are similar in analyses approach by using data in one direction separately for vertical, translational and longitudinal directions.

### 3.1 Transverse, Vertical and Longitudinal motions analyzed separately

Fig. 2 shows displacements in five locations of the deck and their corresponding normalized amplitude spectra. Peaks at  $\sim 0.17\text{Hz}$ ,  $\sim 0.39\text{Hz}$  and  $0.46\text{ Hz}$  are observed. As shown later in the paper,  $\sim 0.46\text{Hz}$  belongs to longitudinal frequency of the towers which are linked to or coupled with the deck via the cables and suspenders. Therefore, this frequency also appears in the vertical and torsional spectra of the deck for the center span as well as other spectra (e.g., transverse) due to coupling.

Fig. 2 (left) shows the TFD for the deck transverse channel CH35 at mid-center span. Other TFDs of transverse channels on the center span are very similar. The figure clearly exhibits the dominance of the lowest frequency mode at  $0.17\text{Hz}$  throughout most of the record starting at about 35s. It also shows a second mode at  $0.98\text{ Hz}$  that is simultaneously active between 35-55s. In Fig. 2 (right), the time history plots exhibit this superposition clearly, particularly for those deck channels at mid-center span (e.g., CH35). The relatively weak amplitude of the frequency at  $0.39\text{ Hz}$  in the TFD is seen more clearly in the spectral plots in Fig. 2 (right). As will be shown later, this frequency is associated with transverse motions of the towers, which are most excited between 60-80 seconds.

Fig. 3 shows cross-spectra, phase and coherency between the three transverse channels (39, 35 and 29) of the center span of the suspension bridge. In the figure, corresponding to three distinct frequencies displayed from cross-spectra plots (and also identified from amplitude spectra), the phase and coherencies are clearly displayed. For example, at  $0.17\text{Hz}$ , CH39, CH35 and CH29 are in phase. At  $0.39\text{ Hz}$ , CH39 and CH35 are in phase, but the phase relationship is not clear for CH39 and CH29. At  $0.98\text{ Hz}$ , CH39 and CH35 are  $180^\circ$  out of phase, as are CH35 and CH29, but CH39 and CH29 are in phase – which means that CH39 and CH29 displace in this mode in the same direction, but both displace in the opposite direction from CH35. From such observations, it is possible to develop unscaled mode shapes (Fig. 3b) keeping in mind that the actual orientation of the sensors is taken as positive direction for these unscaled mode shapes. The modes at  $0.17\text{Hz}$  and  $0.39\text{Hz}$  look similar because of coupling with other modes of the deck and towers, as will be pointed out later in the paper.

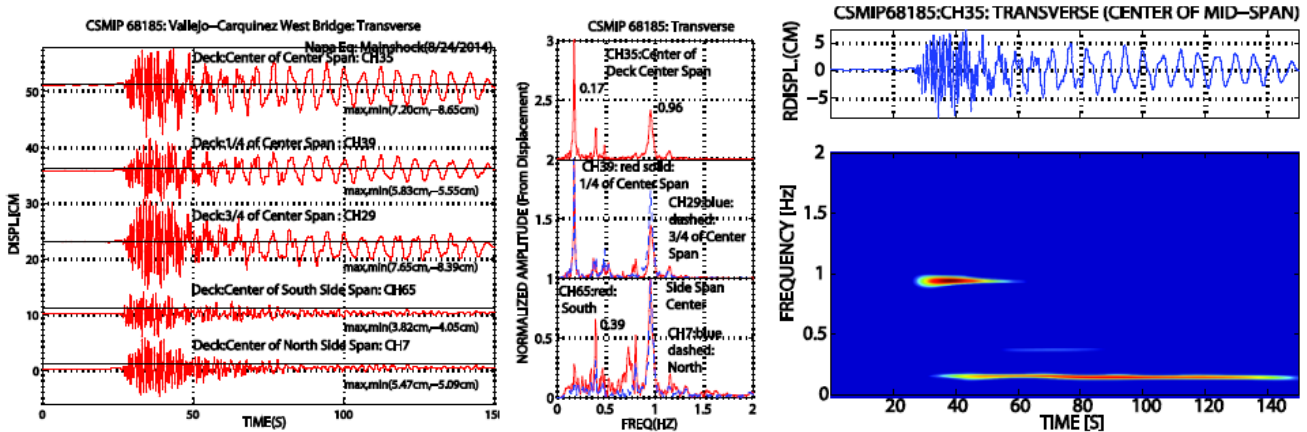


Fig.2 p (left): Deck transverse displacements and corresponding normalized amplitude spectra, (right): Displacement time-history and its TFD for the deck transverse channel CH35 at the middle of the center span clearly exhibits the persistence of the mode at 0.17Hz starting at about 30 s, but also shows that a mode at 0.98 Hz that predominates between ~25-55 s, and a much less pronounced mode at 0.39 Hz (between ~55-85 s).

Fig. 4a shows cross-spectra, phase and coherency between the three transverse channels at the top of two towers, T2 (CH45) and T3 (CH13) and middle of deck center span (CH35). The phase angles and coherencies are displayed again for the first three frequencies (0.17Hz, 0.46Hz and 0.98Hz). Fig. 4b shows unscaled transverse direction mode shapes for the tops of towers, T2 and T3, and middle of deck center span constructed from phase angles. To develop these shapes, displacements at T2 and T3 locations of the deck are assumed to be zero. As before, the positive direction is same as the orientation of each sensor.

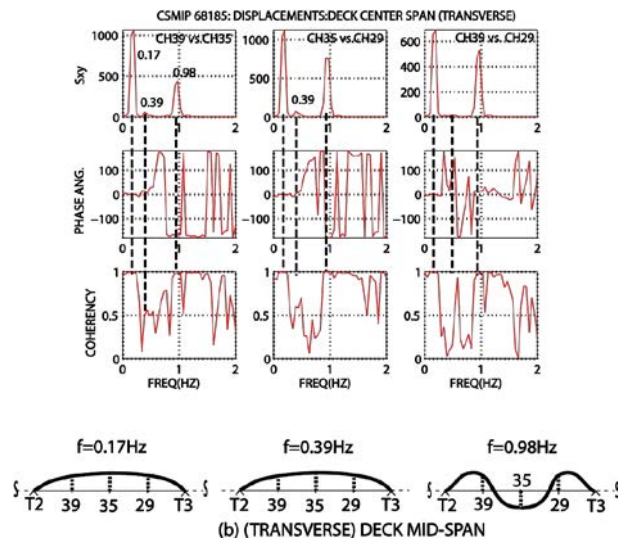
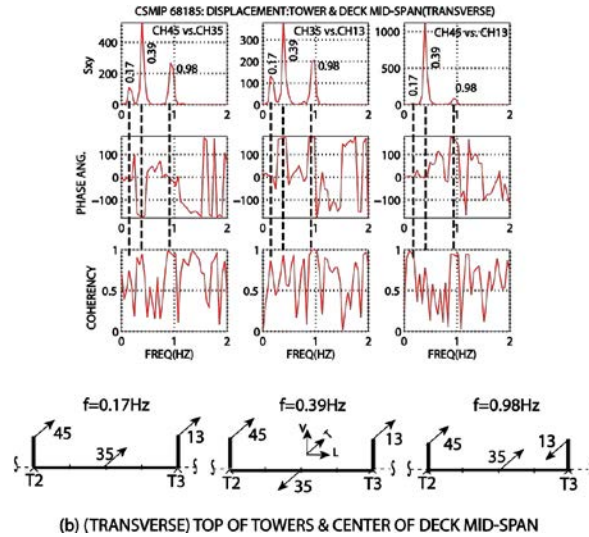


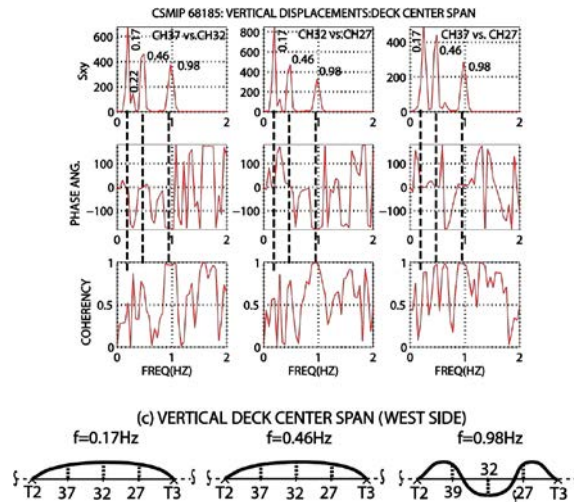
Fig. 3 - (a) Cross-spectra, phase angle and coherency between deck transverse displacements at 1/4 of center span (CH39), middle of center span (CH35) and 3/4 of center span (CH29). Each dashed line identifies the phase and coherency corresponding to a frequency in cross-spectrum. (b) Deck center span transverse mode shapes constructed from phase angles. To develop these shapes, displacements at T2 and T3 locations of the deck are assumed to be zero.



(b) (TRANSVERSE) TOP OF TOWERS & CENTER OF DECK MID-SPAN

Fig. 4 - (a) Cross-spectra, phase angle and coherency between transverse displacements at top of two towers, T2 (CH45) and T3 (CH13) and middle of center span deck (CH35). (b) Top of towers, T2 and T3 and middle of center span deck transverse mode shapes constructed from phase angles. To develop these shapes, displacements at T2 and T3 locations of the deck are assumed to be zero.

Fig. 5a shows cross-spectrum, coherency and phase angle plots of channels 37 versus 32, 32 versus 27, and 37 versus 27. As seen in Fig. 5a, the first modal frequency is 0.17Hz (all in phase, relatively high coherency). All three frequencies are also identified in the figure. Inferred vertical mode shapes for the center span (with zero displacements of deck at tower locations) are provided in Fig. 5b. It is noted that the constructed mode shapes corresponding to 0.17Hz and 0.46Hz are the same as those for the same frequencies of longitudinal motions presented later in the paper. This is due to coupling (or compatibility due to cables and suspenders) between the vertical motions of the deck and longitudinal motions of the tower<sup>4</sup>.



(c) VERTICAL DECK CENTER SPAN (WEST SIDE)

Fig. 5 - (a) Cross-spectra, phase angle and coherency between deck vertical displacements at the ends of the center span, ¼ of center span (CH37), middle of center span (CH32) and ¾ of center span (CH27). (b) Vertical unscaled mode shapes for deck center span with zero displacements of the deck at tower locations.

<sup>4</sup> When considering only the deck center span, modes are defined for 0.17 Hz and 0.46 Hz because we used only center span channels (27,32 and 37). But the same deck center span modes are confirmed when we use CH32 (vertical at middle of deck center span) and longitudinal channels (42 and 10) at the towers. Hence the tower and deck are coupled at each one of the frequencies.



Fig. 6a shows cross-spectra, phase angle and coherency between longitudinal displacements at top of towers, T2 (CH42) and T3 (CH10), and vertical displacement at mid-center span (CH32). Although coherencies are not high, the phase angles are clear (e.g., for 0.17Hz, 180° out of phase between CH42 and CH32, 0° in phase between CH32 and CH10 and with some time-lag, 180° out of phase between CH42 and CH10). Accepting the installed orientation of accelerometers as positive, unscaled mode shapes are constructed in Fig. 6b utilizing the phase angles in Fig. 6a corresponding to the key predominant frequencies displayed. The similarity between the qualitative mode shapes for 0.17Hz and 0.46 Hz is attributable to coupling between modes (e.g., torsional or vertical with quarter-point of mid-span motions included).

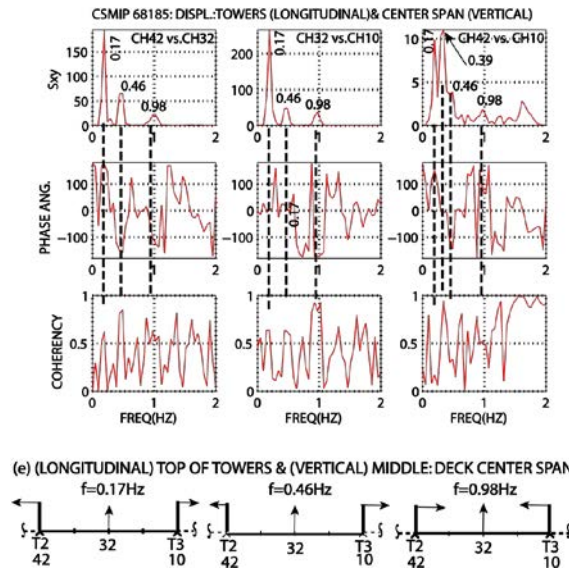


Fig. 6 - (a) Cross-spectra, phase angle and coherency between longitudinal displacements at the tops of towers T2 (CH42) and T3 (CH10), and vertical displacement at mid-center span (CH32). (b) Accepting the installed orientation of accelerometers as positive, unscaled mode shapes are constructed utilizing the phase angles in (a) corresponding to the key frequencies displayed. These modes are coupled with vertical and transverse modes of the deck.

### 3.2 Torsional Motions of Deck and Towers

Torsional behavior and characteristics of key components of the suspension bridge are determined for the deck and towers. In torsion, the deck rotates around the longitudinal axis and the tower rotates around the vertical axis. Torsion of the deck around the longitudinal direction is in phase or out of phase (or out of phase with some time-lag) with one or both of the towers connected by the cables (and suspenders). In the vertical direction, torsion of the deck mid-center span is in phase or out of phase with the quarter point locations of the center span – keeping in mind that the vertical displacement degree of freedom of deck motion at each of the tower locations is constrained. Rotations of the deck around the transverse axis at each of the tower locations is not constrained. Fig. 7 shows relative displacement between two parallel (a) longitudinal channels CH10 and CH11<sup>5</sup> at the top of T3 and (b) vertical channels CH32 and CH33 of the middle of the deck center span. Also shown in the figure are the cross spectrum, phase and coherency of these pairs. The cross-spectrum shows two dominant frequencies that are the same as those determined for both vertical and (or) transverse motions of the deck, and also from the longitudinal motions of the towers. These are also demonstrated in Fig. 8 which shows the TFDs and time-histories of these motions. Fig. 8 also displays beating effects identified in the records.

<sup>5</sup> Only CH10 and CH11 (of T3) are used because CH43 (of T2) did not record and therefore CH42-CH43 cannot be computed.



Fig. 9a illustrates torsion only in the mid-span of the deck. Cross-spectrum, phase angle and coherency between torsional displacements at one-quarter point (CH37-CH38), center (CH32-CH33) and three-quarter point (CH27-CH28) of mid-span of the deck. At 0.46Hz, all cross-spectra are in phase with each other which means all three locations rotate in the same direction around the longitudinal axis. At 0.98Hz, both quarter point locations are in phase but both are 180 out of phase with the center of the mid-span. That means, around the longitudinal axis, the mid-center span is rotating in the direction opposite to both quarter points. For all, coherencies are  $\sim 1$ . Fig. 9b shows unscaled torsional motions of the deck mid-span at both 0.46Hz and 0.98 Hz.

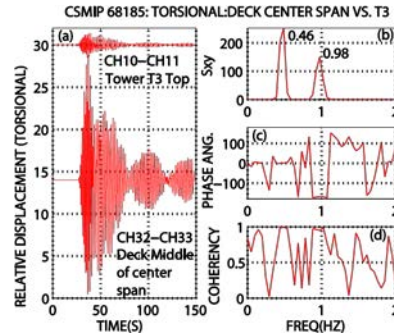


Fig.7 - (a) Relative longitudinal displacements (CH10-CH11) at the top of T3 and vertical displacements (CH32-CH33) at mid-center span of the deck. (b) Cross-spectrum (c) phase angle and (c) coherency between the relative displacements of T2 and the deck.

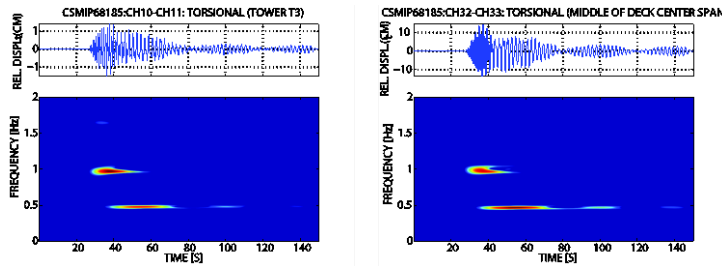


Fig. 8 - Time-history and corresponding TFD of torsional relative displacement (left) at top of T3 (CH10-CH11) and (right) at the middle of the center span (CH32-CH33). Note beating effects.

### 3.3 System Identification

Due to space limitations, detailed description of system identification analyses of the bridge response data is not presented in detail herein. However, the system identification methods used and results are discussed in detail in a separate paper [21]. These results are also used in Table 1 that provides a summary of this study and comparison with previous studies [11-15]. The system identification methods elaborated in the referenced paper used only the free vibration part (90 s) of the 150 second data. Fig. 10 shows the first 4 transverse modes extracted by system identification. In actual case, these are selected from a number of modes that are coupled or closely coupled.

### 3.4 Beating Effect

Beating occurs when repetitively stored potential energy during coupled translational and torsional deformations turns into repetitive vibrational energy. Thus periodic, repeating and resonating motions ensue. The beating becomes severe if the system is lightly damped [8, 22-23]. Time-histories of torsional displacements in both Figs. 7 and 8 exhibit a beating effect with a visually observed period of approximately 40-50 seconds. More on a beating effect from data of this bridge in [21].

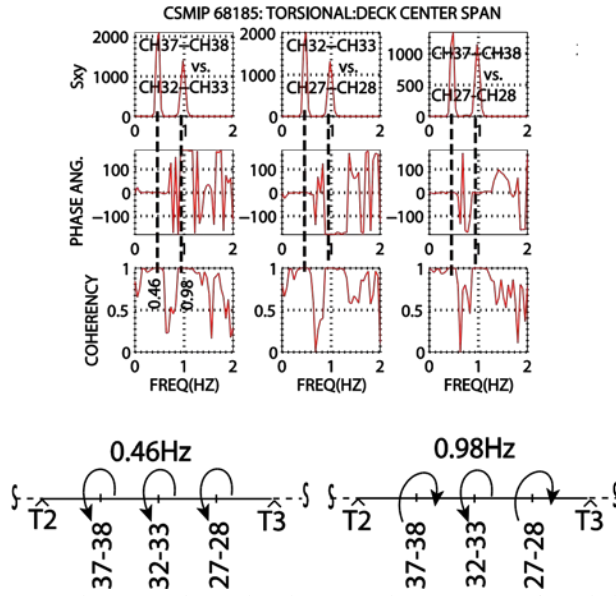


Fig. 9 - (a) Cross-spectrum, phase angle and coherency between torsional displacements at 1/4-point (CH37-CH38), middle (CH32-CH33) and 3/4- point (CH27-CH28) of deck center span. (b) Unscaled torsional modes of deck mid-span.

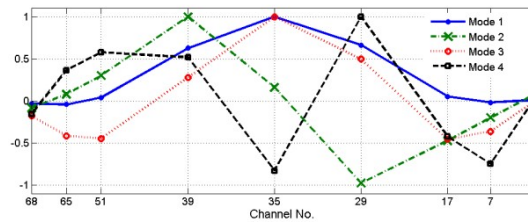


Fig. 10 - Identified transverse mode shapes of the bridge deck (90 s of free vibration part of the 150 s transverse data recorded at 9 locations of the deck used).

#### 4. Discussion and Comparison with previous studies

Table 1 provides comparison between natural frequency and damping ratios of the bridge deck in transverse, vertical longitudinal directions identified in this study with those identified by other researchers. As stated earlier, this study is the first study (a) that utilized earthquake response data and (b) that also included data related to the response of the towers in an earthquake. For example, we identified Tower's frequencies in transverse, vertical, longitudinal, and torsion directions as 0.39Hz, 0.17/0.46Hz<sup>6</sup>, 0.46Hz, and 0.46 Hz, respectively. Corresponding transverse and longitudinal modal damping ratios of the towers are 1.73% and 6.5%, respectively.

As seen in Table 1, natural frequencies are quite similar in all three cases (this study and [11, 15]). This is expected because we did not observe any nonlinearity in the system. Damping ratios of this study are close to those reported by Hong et al. [15] but quite different from those reported by Conte et al. [11]). While the level of vibration in the earthquake was quite larger than ambient data used by Hong et al. [15], this similarity in the damping ratio is an important observation that vibrational energy attenuation does not alter significantly during the higher level amplitudes in the responses of the bridge during the earthquake as compared to ambient response assessment.



**Table 1.** Comparison of dynamic characteristics of the Carquinez Strait suspension bridge. (Although, vertical frequency of the tower is outside of the scope of this study, two of the prominent frequencies 0.17 Hz and 0.46 Hz are identified in the vertical spectra of vertical motions of the towers. This is attributable to the effect of cable on top of towers).

Predominant Frequencies (Hz) and damping (%)				
Orientation	Trans.	Vert.	Long.	Torsion
This study (results from spectral analyses)				
Deck Freq. [Hz]	0.17	0.17	N/A but coupled with tower at 0.17 and 0.46 Hz	Coupled with vertical and transverse
Deck Damp. (%)	0.61	5.17	-	-
Tower Freq. [Hz]	.39	0.17*/0.46*	0.46	0.46
Tower Damp. (%)	1.73	-	6.5	
Other studies (Conte et al., 2008 [11])				
Deck Freq. [Hz]	0.16	0.194		0.47
Results from Hong et al. (2011) [15] reported here				
Deck Freq. (Hz)	0.17	0.19		0.17
Deck Damp. (%)	1.21	7.0	-	1.21

## 5. Conclusions

The response data recorded by a seismic array on the suspension bridge at Carquinez Strait, CA, during the 24 August 2014 South Napa, CA, earthquake are analyzed. Such data that allow identification of behavior of a suspension bridge during a seismic event are scarce. It should be noted that, for this bridge, the only recorded event data from a single azimuth were used in the current study. It is likely that the Carquinez Strait suspension bridge may indicate azimuthally-dependent responses during future earthquakes (e.g., from the Hayward Fault).

None of the previous studies (of this bridge) interpreted their results in terms of coupled modes while, in our study, coupling of modes is concluded to be an important behavioral aspect. In addition to identifying mode coupling a beating effect is found to be an important behavioral characteristic that may influence its performance. Beating may add to low-cycle fatigue and may lead to persistent resonance.

It is also shown that the frequencies as well as phase angles corresponding to the frequencies all computed by spectral analyses are useful for constructing unscaled mode shapes. Coherencies in most cases are good (~1), but some are less. In some cases, phases also show some deviation, most likely due to time-lag. The coupling occurs between the transverse, vertical, longitudinal and torsional modes of the deck center span and towers. Because of the low frequency of the deck relative to that of the tower, the deck frequency is dominant, as exhibited by appropriate spectra (e.g., spectrograms). The spectrograms show that the significant modes of the bridge are superimposed. Furthermore, basin effects should also be considered for larger magnitude earthquakes expected south of the bridge (e.g., Hayward Fault) that may have significantly larger input motions with lower frequency content in the band of the lower frequencies of the bridge.

Finally, the earthquake response data analyzed herein reveal significant behavioral aspects for the Carquinez Strait suspension bridge that were not revealed previously by lower amplitude ambient data or mathematical modeling. As such, the earthquake response data indicate that coupling and beating phenomena associated with various components of the bridge need to be considered in mathematical models to better account for the observed response of the bridge.

## 6. Acknowledgments

The authors thank the informational support they received from Anthony Shakal, Hamid Haddadi and Mo Huang (all CSMIP) and from Pat Hipley (Caltrans). Any use of trade, firm, or product names is for descriptive purposes only and does not imply endorsement by the U.S. Government.



**7. Data Source and Copyrights:** [www.strongmotioncenter.org](http://www.strongmotioncenter.org) (Last visited January 5, 2016). Several figures used in this paper are from a lengthy paper (Reference 21 in review by Earthquake Spectra, a journal of EERI. Earthquake Spectra allows authors to use their own figures without permission.

## 8. References

- [1] EERI Special earthquake Report: M6.0 South Napa Earthquake of August 24, 2014 (2014): in EERI Newsletter, October 15, 2014, 27 pages.
- [2] Abdel-Ghaffar A, Scanlan R (1985a): Ambient vibration studies of Golden Gate Bridge: suspended structure, *Journal of Engineering Mechanics*, 111, 463–482.
- [3] Abdel-Ghaffar A, Scanlan R (1985b): Ambient vibration Studies of Golden Gate Bridge: II. pier-tower structure, *Journal of Engineering Mechanics*, 111, 483–499.
- [4] Vincent GS (1958): Golden Gate Bridge vibration studies, *Journal of Str. Div.*, ASCE, 84, Paper 1817.
- [5] Vincent GS (1962a): Correlation of predicted and observed suspension bridge behavior, *Transactions*, ASCE, 127, 646–666.
- [6] Vincent GS (1962b): Golden Gate Bridge vibration studies, *Transactions*, ASCE, 127, 667.
- [7] Çelebi M (2012): Golden Gate Bridge Response: A Study with Low-Amplitude Data from Three Earthquakes, *Earthquake Spectra*, Volume 28, No. 2, pages 487–510, May 2012.
- [8] Çelebi M (2006): Real-time seismic monitoring of the new Cape Girardeau (MO) Bridge and Preliminary analyses of recorded data: An Overview, *Earthquake Spectra*, 22, 3, August 2006, pp.609-630.
- [9] Siringoringo DM, Fujino Y, Namikawa K (2014): Seismic Response Analyses of the Yokohama Bay Cable-Stayed Bridge in the 2011 Great East Japan Earthquake. *Journal of Bridge Engineering ASCE*, 2014, 19(8):A4014006.
- [10] Siringoringo DM, Fujino Y (2006): Observed dynamic performance of the Yokohama-Bay Bridge from system identification using seismic records. *Structural Control and Health Monitoring*, Special Issue: Thomas K. Caughey Memorial Issue, 13(1), 226–244.
- [11] Conte JP, He X, Moaveni B, Masri SM, Caffrey JP, Wahbeh M, Tasbihgoo F, Whang DH, Elgamal A.(2008): Dynamic Testing of Alfred Zampa Memorial Bridge, *Jour. of Str. Eng.*, ASCE, 134, 6, 1006-1015.
- [12] He X, Moaveni B, Conte JP, Elgamal A, Masri SM. (2009): System Identification of Alfred Zampa Memorial Bridge Using Dynamic Field Test Data, *Journal of Str. Eng.*, ASCE, 135,1, 54-63.
- [13] Nayeri MRD, Tasbihgoo F, Wahbeh M, Caffrey JP, Masri SF, Conte JP, Elgamal A. (2009): Study of Time-Domain Techniques for Modal Parameter Identification of a Long Suspension Bridge with Dense Sensor Arrays, ASCE *Journal of Engineering Mechanics*, 135,7,669-683.
- [14] Betti R, Hong AL, (2008): Identification of the baseline parameters of the Carquinez Suspension Bridge using ambient vibration data, PROC. State of Calif., California Geological Survey, SMIP08 Seminar 63-81.
- [15] Hong AL, Ubertini F, Betti R,(2011): Wind Analysis of a Suspension Bridge: Identification and Finite-Element Model Simulation ASCE *Journal of Structural Engineering*, 137,1,133-142.
- [16] Nayeri MRD. (2007): Analytical and Experimental Studies in System Identification and Modeling for Structural Control and Health Monitoring, PhD dissertation, Univ. of So. California, 207 pages.
- [17] Bendat JS, Piersol AG,(1980): *Engineering Applications of correlation and spectral analyses*, John Wiley and sons, New York, N.Y. 302 p.
- [18] Auger F, Flandrin P.(1995):Improving the readability of time-frequency and time-scale representations by the reassignment method, *IEEE Transactions on Signal Processing*, 43, 1068-1089.
- [19] Shakal A, Haddadi H, Huang M, Stephens C. (2014): Highlights of Strong-Motion Data from the M6.0 South Napa Earthquake of August 24, 2014, PROC *SMIP2014 Seminar on Utilization of Strong Motion Data*, October 9, 2014, Berkeley, CA. 111-129.
- [20] Auger F, Flandrin P, Goncalves P, Lemoine O, (1996): Time-Frequency Toolbox for use with MATLAB, Tutorial, CNRS (France) and Rice University ([www.nongnu.org/tftb/tutorial.pdf](http://www.nongnu.org/tftb/tutorial.pdf); last accessed September 10, 2013), pp. 150.
- [21] Çelebi M, Ghahari SF, Taciroglu E. (2016): Responses of the Odd Couple Carquinez, CA Bridges During the M6.0 South Napa Earthquake of August 24, 2014: Suspension Bridge,in review, *Earthquake Spectra*.
- [22] Boroschek, R. L., and Mahin, S. A., (1991). Investigation of the Seismic Response of a Lightly Damped Torsionally Coupled Building, Report *UCB/EERC-91/18*, University of California, Berkeley, 291 p.
- [23] Boroschek, R. L., Mahin, S. A., and Zeris, C. A., (1990). Seismic Response and analytical modeling of three instrumented buildings, in PROC. 4<sup>th</sup> U.S. National Conf. on Eq. Eng., Palm Springs, Ca.,2, 219-22